Carbohydrate Polymers 85 (2011) 885–894

Contents lists available at ScienceDirect

Carbohydrate Polymers

journal homepage: www.elsevier.com/locate/carbpol

Biomimetic multicomponent polysaccharide/nano-hydroxyapatite composites for bone tissue engineering

Junjie Li[a,c], Hong Sun[b], Da Sun[a], Yuli Yao[b], Fanglian Yao[a,*], Kangde Yao[c]

[a] Department of Polymer Science and Key Laboratory of Systems Bioengineering of Ministry of Education, School of Chemical Engineering and Technology, Tianjin University, Tianjin 300072, China
[b] Department of Basic Medical Sciences, North China Coal Medical College, Tangshan 063000, China
[c] Research Institute of Polymeric Materials, Tianjin University, Tianjin 300072, China

ARTICLE INFO

Article history:
Received 5 October 2010
Received in revised form 6 April 2011
Accepted 8 April 2011
Available online 15 April 2011

Keywords:
Polysaccharide
Multicomponent
Nano-hydroxyapatite
Scaffold
Bone tissue engineering

ABSTRACT

Nano-hydroxyapatite/chitosan–pectin (nHCP) composite was prepared via mineralization of a chitosan–pectin network. Then nHCP/chitosan–gelatin (nHCP/CG) scaffolds were prepared via the blending of nHCP and chitosan–gelatin solution. Results suggested that nHCP/CG scaffolds have appropriate porosity, water absorption ability and degradation behaviors. nHCP can be fused into the pore wall of nHCP/CG scaffold via chemical crosslinking interactions, which avoids the agglomeration and migration of nHA particles. Moreover, the compressive strength of nHCP/CG scaffold ranges from 10.4 ± 1.64 to 13.5 ± 3.85 MPa. nHCP/CG scaffolds have stable physical and chemical structures, which can provide appropriate microenvironments for cells to attach and proliferate for MC 3T3-E1 cells. Therefore, nHCG/CG is a potential biomaterial in bone tissue engineering.

1. Introduction

Three-dimensional (3D) nHA/polymer scaffolds constitute a particularly large and interesting group in bone tissue engineering due to their similar structures to nature bone. An ideal nHA/polymer composite involved in bone-repair scaffold should be biodegradable, mechanically robust and biocompatible. The composites should also facilitate early mineralization and support new bone formation, while at the same time, allow for the replacement by new bone (Cui, Li, & Ge, 2007). Some natural polysaccharides (chitosan, pectin, alginate, etc.) and proteins (collagen and gelatin) have been investigated because of the similarity of their structures and biocompatibility. Chitosan has a hydrophilic surface promoting cell proliferation and differentiation (Suh & Matthew, 2000). Chitosan scaffolds are osteoconductive and are able to enhance bone formation both in vitro and in vivo (Di Martino, Sittinger, & Risbud, 2005; Khor & Lim, 2003). Pectin is a plant polysaccharide primarily obtained from edible plants, which is enriched in galacturonic acid and galacturonic acid methyl ester units. The carboxyl groups of pectin play important roles in the process of mineralization, which have a catalytic effect for heterogeneous apatite nucleation. Pectin can provide mechanical strength for cell walls of higher plants as well as play important roles in various cellular processes (Kokkonen et al., 2008; Liu, Fishman, Kost, & Hicks, 2003). Recently, pectin has also been investigated for possible applications in bone tissue engineering (Liu et al., 2004). Gelatin is a partially denatured derivative of collagen, which has the potential to support the growth of osteoblasts and promote bone regeneration in defective areas (Rohanizadeh, Swain, & Mason, 2008). The morphology and structure of the nHA crystals could be modulated by these natural polymers if the nHA crystals were formed in situ in these polymer solutions.

nHA/polymer nanocomposites have been synthesized via blending the nHA particles and polymer (Kim, Kim, & Salih, 2005; Kim, Knowles, & Kim, 2005). Such nHA/polymer nanocomposites exhibit excellent physicochemical properties which appear to make them a suitable candidate to be used as a supportive structure for cells functions (Nejati, Firouzdor, Eslaminejad, & Bagheri, 2009; Zhao et al., 2002). However, the nHA particles in this case did not disperse well as they agglomerate easily and even settle. As a result it is difficult to form a controlled structure (Kim, Kim, et al., 2005; Kim, Knowles, et al., 2005) through preparation by blending. Meanwhile, nHA crystals may migrate from the composites because of the weak interactions between nHA particle and polymer. When cells interact with the composites, the interfaces between nHA crystals and polymers were destroyed and nHA crystals were easily released from the polymer matrix. This defect may cause a large decrease in the mechanical strength. In order to enhance the interactions between nHA crystals and polymers, the nHA/polymer composites were prepared via mineralization

* Corresponding author. Tel.: +86 22 27402893; fax: +86 22 27403389.
E-mail addresses: yaofanglian@tju.edu.cn, ripm@tju.edu.cn (F. Yao).

0144-8617/$ – see front matter © 2011 Published by Elsevier Ltd.
doi:10.1016/j.carbpol.2011.04.015

using simulated body fluid (SBF) or Ca/P solutions. The nHA crystals formed on the surface of preformed polymer matrices. This method could effectively modulate the size of nHA crystals when different polymer matrices were used (Li, Chen, Yin, Yao, & Yao, 2007; Yin et al., 2004). The nHA/polymer nanocomposite obtained by surface mineralization is a suitable substrate for the distribution, attachment and migration of osteoblast-like cells. It also accelerates the osteogenic differentiation at an early stage and promotes ECM formation (Manjubala, Ponomarev, Wilke, & Jandt, 2008; Manjubala, Scheler, Bossert, & Jandt, 2006). However, the polymer matrices are covered gradually by nHA crystals along with the formation of nHA. As a result, effects of polymer matrices on cell functions are limited to the short time when cells contact the uncoated surfaces. Therefore, it is a challenge to develop a new way for the preparation of nHA/polymer bulk composites, which could protect the nHA crystal from self-aggregation and improve the homogeneous distribution of nHA crystals in the composites scaffold, to take the place of surface mineralization

In our previous research, the HA/chitosan–gelatin (HCG) composite scaffolds were prepared via directly dispersing HA particles into chitosan–gelatin matrix. The HCG composites showed excellent histocompatibility, but the HA particles are heterogeneous in chitosan–gelatin matrix (Zhao et al., 2002). On the other hand, the homogeneous nHA coating could be formatted on the surface of chitosan–gelatin network, and the nHA/chitosan–gelatin network films could improve the attachment, proliferation and differentiation of mesenchymal stem cells (MSCs) (Li et al., 2009). However, owing to the directly contact with the nHA coating, the chitosan–gelatin matrix of the composite has little affected on the behavior of MSCs. In this study, in order to overcome these disadvantages, the multicomponent polysaccharide/nano-hydroxyapatite composites were prepared using chitosan, gelatin and pectin as the organic matrix. First, the nHA/chitosan–pectin (nHCP) composites were prepared via mineralization. Then, for the preparation of multicomponent nHCP/CG bulk composite films and scaffolds, the nHCP was blended with chitosan–gelatin (CG) solutions. The crosslinking reaction between nHCP and CG network were carried out using glutaraldehyde as the crosslinking agent. Here, nHA was introduced to the scaffold in the form of nHCP that could improve the dispersion uniformity and stability of nHA crystal in CG matrix. The crosslinking reaction between nHCP and CG network also plays an important role in this. The suitability of the nHCP/CG nanocomposite scaffold for tissue engineering is described in terms of microstructure, physicochemical and mechanical properties. Moreover, the response of mouse pre-osteoblasts (MC 3T3-E1) to the multicomponent nHCP/CG nanocomposite was assessed. As controls, the nHA/CG composites are also prepared via directly blending nHA particles and chitosan–gelatin solutions.

2. Materials and methods

2.1. Materials

Chitosan (CS, mean molecular weight 2.0×10^5 Ad, deacetylation, >85%) was supplied by Qingdao Medical Institute (Qingdao, China). Pectin (citrus-derived) and gelatin were purchased from Sigma Chemical Co. (St. Louis, MO). All other reagents used were of analytical grade.

2.2. Preparation and characterization of nano-hydroxyapatite/chitosan–pectin composites

The synthesis of nHCP composites has been reported previously (Li, Kommareddy, et al., 2010; Li, Zhu, et al., 2010). Chitosan was dissolved in acetic acid solution (1% v/v) and pectin was dissolved in deionized water. Then the $Ca(NO_3)_2$ was added into pectin solution and NaH_2PO_4 was added into chitosan solution, at molar ratio Ca/P = 1.67. After 5 h, the NaH_2PO_4/chitosan solution was added dropwise into $Ca(NO_3)_2$/pectin solution with magnetic stirring. The pH value was adjusted to 13. After 48 h, the precipitate was separated by centrifugation and washed with deionized water until the pH value reached 7.0. Further, the precipitate was lyophilized and the nHCP composites containing 66.7% (wt%) nHA crystals were obtained. All these steps except lyophilization were conducted at room temperature.

The phase composition of as-prepared powders is determined using X-ray diffraction (XRD) (Rigaku D/max 2500v/pc). The crystallite morphology of the nHCP composites was observed by a Transmission Electron Microscope (TEM, JEM-100CX II, Japan).

2.3. Preparation and characterization of multicomponent nHCP/CG composite film and scaffold

2.3.1. Preparation of multicomponent nHCP/CG composites film and scaffold

Chitosan and gelatin were dissolved in 1% (v/v) acetic acid solution and water respectively and mixed together. The nHCP composite powders were ultrasonically dispersed (800w) in chitosan–gelatin (CG) solution for 10 min. A suitable amount of glutaraldehyde aqueous solution (0.25 wt%) was incorporated into the nHCP/CG dispersion at a magnetic stirrer and the mixture was transferred to polystyrene Petri Dishes. After drying at room temperature, a film with ca 0.1 mm thickness was obtained. The scaffolds were prepared by freezing the dispersion mixture at −50 °C for 24 h and lyophilized in a freeze dryer. In order to neutralize the residue of acetic acid in films and scaffolds, this was followed by treatment with NaOH solution (1%(wt%)) and washing with deionized distilled water to pH = 7.0. Then, the samples were retreated with sodium borohydride ($NaBH_4$) solution to eliminate the residual glutaraldehyde. The films and scaffolds were repeatedly washed with deionized water and normal saline for cell culture studies. Finally the films were dried at room temperature and scaffolds were lyophilized again. The fraction of nHCP in the nHCP/CG multicomponent composites were 0 (pure CG composites), 10, 30, and 50 wt% respectively.

As controls, nHA/CG composite film or scaffold were also prepared in the same way. The fraction of nHA particle in nHA/CG composite is 50 wt%.

2.3.2. Interactions in nHCP/CG multicomponent composite

The interactions among each component in nHCP/CG and nHA/CG composites were investigated by a FTIR spectrometer. Dried composites were ground after embrittlement using liquid nitrogen and mixed thoroughly with potassium bromide at a ratio of 1:5 (Sample: KBr). The IR spectra were then analyzed using MAGNA-560 (Nicolet, USA) operating at the range of 400–4000 cm^{-1}.

2.3.3. Microstructure of scaffold

The morphology of the scaffold was observed by SEM (XL30, PHILIPS, The Netherlands). The scaffold was coated with gold using a sputter coater (DeskII, Denton vacuum Inc.). During the process of gold coating, the gas pressure was kept at 50 mtorr, and the current was 20 mA. The coating time was 300 s. Samples were analyzed at 10 kV.

2.3.4. Water absorption of scaffold

Three dry scaffolds from each group were weighed and immersed in 10 ml water at 37 °C. At various time intervals, the scaffolds were carefully taken out and wiped with filter paper to

remove surface water followed by measurement of the wet weight of the sample. The water absorption was calculated using the Eq. (1), where M_w and M_o are the wet and dry weight of the sample, respectively.

$$\text{Water absorption } (\%) = 100\frac{M_w - M_o}{M_o} \quad (1)$$

2.3.5. Degradation behavior of scaffold

The degradation ability of the scaffold was evaluated using a lysozyme degradation test. In this test, degradation profiles of 3D scaffolds were plotted after incubation in PBS including lysozyme (30,000 U/ml) at 37 °C air bath and observed for 11 weeks. At 1, 3, 5, 7, 9 and 11 week, triplicate specimens for each sample were removed and washing with deionized water. The weight (wt) of sample was measured after lyophilization. The weight remaining was evaluated using the following Eq. (2).

$$\text{Weight remaining } (\%) = 100\frac{M_t}{M_o} \quad (2)$$

2.3.6. Mechanical strength of film and scaffold

The tensile strength of the multicomponent composite films was evaluated using mechanical instrument (M350-10KN, Testometric, England) equipped with fixed grips lined with thin rubber on the ends. The initial grip separation was set at 40 mm, and the crosshead speed was 1 mm/s. The tensile strength was determined from stress–strain curves obtained from uniaxial tensile tests.

Compressive modulus of scaffolds was measured using mechanical instrument (M350-10KN, Testometric, England). All samples were column (16 mm in diameter and 12 mm in thickness). A crosshead speed of 1 mm/min was used. The compressive modulus is defined as the initial linear modulus on the stress/strain curves. Six specimens were tested for each sample. The averages and standard deviations were reported.

2.4. Response of pre-osteoblasts (MC 3T3-E1) to nHCP/CG multicomponent composite

2.4.1. Cell attachment behaviors on nHCP/CG films

In order to evaluate the initial cell adhesion performance of the multicomponent nHCP/CG 2D films, cell attachment studies were conducted. The pre-osteoblasts MC 3T3-E1 were seeded (1×10^5 cells per well) on prewetted nHCP/CG, CG and nHA/CG films in 24-well tissue-culture plates. DMEM supplemented with 10% FBS was used. At 1, 2, 4, 6 and 8 h, the MTT assay was measured to evaluated the attachment ability of MC 3T3-E1 on the films. Briefly, at corresponding time points the cell viability was evaluated using the MTT assay, in which 50 μl of MTT (Sigma, 5 mg/ml in Dulbecco's PBS) was added to each well and incubated at 37 °C, 5% CO_2 for 4 h. After removal of the medium, the converted dye was dissolved in acidic isopropanol (0.05 M HCl in absolute iospropanol). Solution (100 μl) of each sample was transferred to a 96-well plate. The absorbance of converted dye is measured at a wavelength of 570 nm using an enzyme-linked immunosorbent assay (ELISA) plate reader (TECAN SPECTRA |||).

2.4.2. Cell proliferation behaviors on nHCP/CG film and scaffold

The pre-osteoblasts MC 3T3-E1 were seeded (1×10^4 cells per well) on prewetted nHCP/CG, CG and nHA/CG films in 24-well tissue-culture plates. DMEM supplemented with 10% FBS was used for cell proliferation of MC 3T3-E1. At day 1, 4, 7, 10 and 14 the MTT assay was measured to investigate the proliferation viability of MC 3T3-E1 on the film.

Approximately 8×10^5 cells were seeded into each multicomponent CG, nHCP/CG (50 wt%) and nHA/CG (50 wt%) 3D dry scaffolds in 24-well tissue-culture plates and 500 μl DMEM cell cultivation solution containing 10% FBS was added into each well. The proliferation behaviors of MC 3T3-E1 in the 3D scaffolds at day 7, 14 and 21were evaluated using MTT assay.

2.4.3. Cell morphology on multicomponent composite film and scaffold

A 500 μl cell suspension was seeded on the top of multicomponent 2D films (ca 3.0×10^4 cells) and 3D scaffolds (ca 8.0×10^5 cells) in 24-well tissue culture plates. At certain time points, the cell-scaffold constructs were incubated with dye (0.02 mg/ml of PBS) for 3 min at room temperature, and then the cell-film and cell-scaffold constructs were washed using PBS. Cell-scaffolds constructs were directly viewed under a microscope to detect fluorescence at the excitation and emission wavelengths of 490/520 nm. Transfected cells appeared as green fluorescence. Meanwhile, after the MC 3T3-E1 were cultured for 3–21 days at 37 °C and 5% CO_2, the cell-film samples were fixed with 2.5% glutaraldehyde in 0.1 M PBS (pH 7.2). The specimens were then dehydrated through a graded series of ethanol, vacuum dried and gold coated for scanning electron microscopy (SEM, XL30, PHILIPS, The Netherlands) observation.

2.5. Statistical analysis

Statistical analysis was performed with the OriginPro Software for Windows. Results of cells viability were reported as mean standard deviation for $n = 4$, and the differences among the samples were tested by Student's t-test with a significance level of $p < 0.05$ or $p < 0.01$.

3. Results and discussion

3.1. Characterization of nHCP composite

The diffraction peaks at 26.0°, 31.8°, 32.9°, 39.8° and 46.7° could be defined in XRD patterns (Fig. 1(A)). All of those are consisted with the ICDD standard card of HA, which implied that the crystal phase in the samples is only HA without detecting other impurity although the broadening and overlapping of peaks appeared due to the poor crystallinity. That is to say, the HA crystal were formed in chitosan–pectin system, and the size is ca. 15.8 nm which is very similar to the value of apatite of natured bone (18.6–16.4 nm). Moreover, the nHA crystals were embedded in chitosan–pectin matrices (cf. Fig. 1(B)). Our previous research (Li, Kommareddy, et al., 2010; Li, Zhu, et al., 2010) found that the chitosan–pectin polyelectrolyte complex (PEC) networks play very important roles in the formation of nHA crystal, the formation and dissociation of chitosan–pectin PEC could modulated the nucleation and growth of nHA crystals via adjusting pH values. Moreover, the dispersion of nHCP composite has a good stability when chitosan/pectin ratio $\leqq$1:1. These characteristics give nHCP have more obvious advantages compared with naked nHA particles when preparing homogeneous 3D porous scaffolds.

3.2. Combination of nHCP and chitosan–gelatin network

As shown in Fig. 2(A), the IR absorption at 1669 cm^{-1} of nHA/CG composites can be attributed to COOH groups of gelatin of nHA/CG. It shifted to the direction of higher wavenumbers compared with COOH groups (1660 cm^{-1}) of CG matrix. This suggested the formation of hydrogen bond or polar interactions between nHA crystalline and CG matrix (Fig. 2(B)). These interactions may also exist between nHCP and CG matrix because the absorption of COOH of nHCP/CG appeared at 1664 cm^{-1}. Li et al. (Cheng et al., 2009) found that hydrogen bonds may also existed between $-NH_2$ of CG matrices and OH groups of HA. These interactions may have occurred similarly to those occurring between the components of

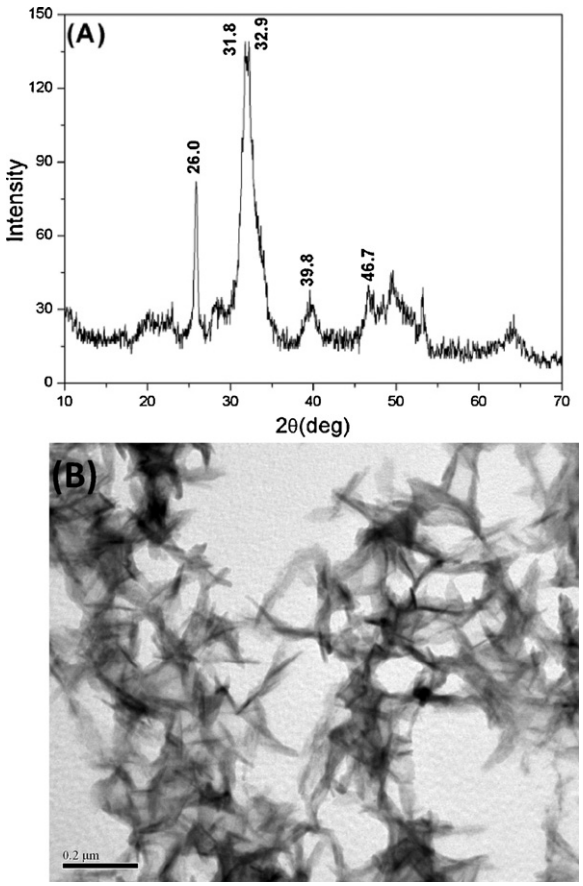

Fig. 1. XRD patterns (A) and TEM image (B) of nHCP composites.

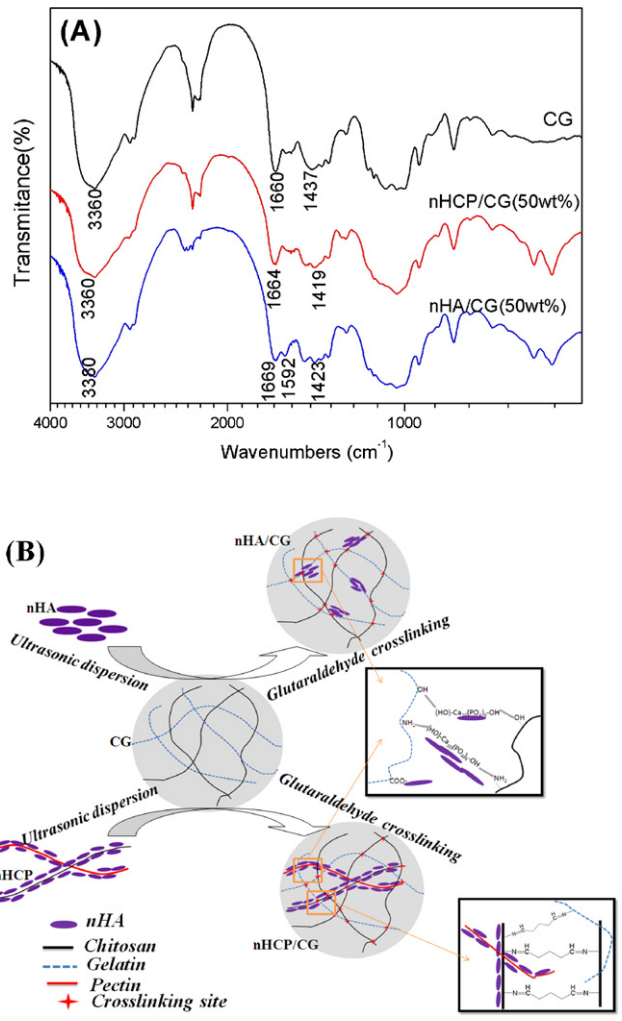

Fig. 2. (A) FTIR spectra of CG, nHCP/CG (50 wt%) and (c) nHA/CG (50 wt%); (B) scheme of the formation process of nHCP/CG and nHA/CG composites, illustrating the interactions between CG matrix and nHCP, and between CG and naked nHA.

bone (Thein-Han & Misra, 2009). Moreover, the absorption bands of amino group at 1539, 1541 cm^{-1} which appear in gelatin and chitosan respectively, have become very weak or even disappeared in the CG, nHCP/CG and nHA/CG composites. It is believed that this results from Schiff base reaction between the amino groups of chitosan or gelatin and aldehyde groups of glutaraldehyde. Therefore crosslinking reaction may occur not only between chitosan and gelatin but also between nHCP composites and chitosan and/or between nHCP composites and gelatin because the unreacted side groups ($-NH_2$) of nHCP powder still exist (cf. Fig. 2(B)). That is to say, the nHCP composites could combine with CG matrix through chemical crosslinking reaction. This is the main reason why nHCP could homogenously distribute in the CG network and remain their stability for a long time.

3.3. Microstructure of the nHCP/CG scaffold

The microstructure and pore size distribution of scaffolds significantly affect cell proliferation, migration and function in bone tissue engineering, as well as vascularization. The importance of porosity for bone tissue engineering has been consistently demonstrated. The porosity parameter directly controls the mass transfer of nutrients and metabolic waste products to cells as well as assists cell migration and vascularization, all of which are essential factors for new bone formation. The porosity of nHA/CG (50 wt%) scaffold ($70.8 \pm 1.26\%$) is lower than that of nHCP/CG (50 wt%) scaffold ($79.2 \pm 3.32\%$). Moreover, the porosity of nHCP/CG scaffold decreased with the increasing of nHCP contents in multicomponent nHCP/CG system.

Fig. 3 shows SEM images of the nHCP/CG and nHA/CG porous scaffolds prepared by the freeze-drying method. The resulting 3D scaffolds have hierarchical porous structures with well-controlled interconnected pores. The average pore diameters range from 100 to 200 μm. The nHCP composites are fused to pore wall of scaffold, especially for nHCP/CG (50 wt%). However, the agglomerates of nHA particles can be significantly observed in nHA/CG scaffolds. Most of nHA particles located on the surface of pore wall (Fig. 3(E)). These findings might due to the different dispersion stability of nHCP and nHA in chitosan–gelatin solution. There are strong binding of Ca^{2+} with COO– of pectin, which results in more PO_4^{3-} expose on the surface of nHA crystal. The high surface negative charges can avoid the coalescence phenomena of nHCP composites and make the nHCP composites homodisperse in CG matrix (Li et al., 2009). As for nHA/CG scaffold, the situation is quite different, the naked nHA particles were easy to agglomerate and could not well disperse in CG solution, even settled, which made it difficult to form a homogeneous structure during the formation of nHA/CG scaffold (Kim, Kim, et al., 2005; Kim, Knowles, et al., 2005). Most importantly, the binding mode of CG matrices with nHCP in nHCP/CG scaffold and naked nHA in nHA/CG scaffold is different. Although, there are ionic or polar interactions and hydrogen bonds between nHA and CG matrix in both nHCP/CG and nHA/CG composites. However, the chemical crosslinking between CG matrix and nHCP powder only exists in nHCP/CG scaffolds, which makes nHCP combine with CG matrix more tightly than naked nHA.

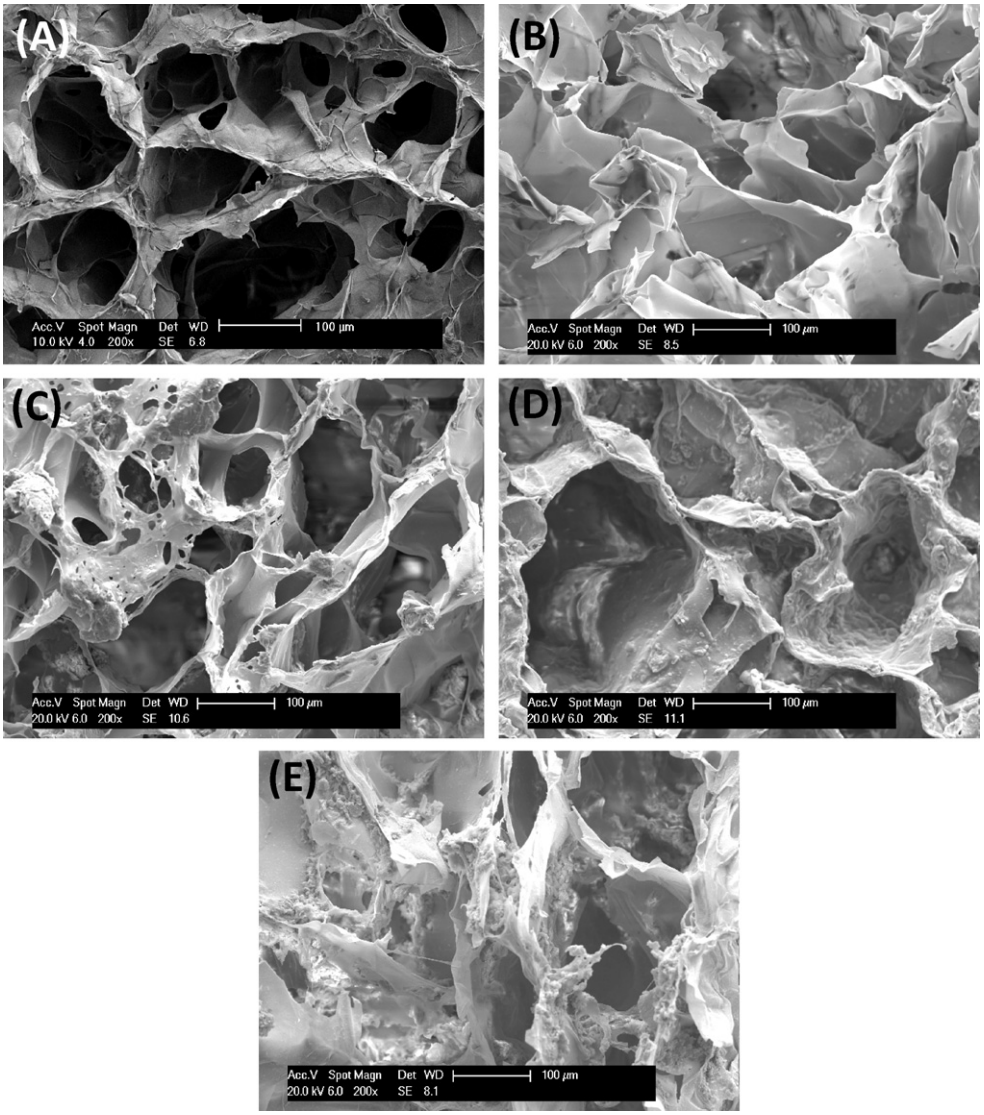

Fig. 3. SEM images illustrating the microporous structure of (A) CG, (B) nHCP/CG (10 wt%), (C) nHCP/CG (30 wt%), (D) nHCP/CG (50 wt%) and (E) nHA/CG (50 wt%).

3.4. Water absorption and degradation of nHCP/CG scaffold

The hydrophilicity of scaffolds is one of the most critical features in the evaluation of biomaterials for tissue engineering which is important for the absorption of body fluid and for a transfer of cell nutrients and metabolites. Results suggested water absorption increases rapidly within the initial 2 h, and the water absorption further increase and attains an equilibrium state within 10 h due to its compact 3-D scaffolds structure, which allow slow entry of water molecules into their inner core (Mandal, Priya, & Kundu, 2009). All specimens could bind 1000–1900-fold of water and still entirely maintain their form, which indicates that these 3D scaffolds have excellent hydrophilicity. Scaffolds containing nHCP have lower water absorption than pure CG scaffold, and the water absorption ability decrease with the increasing of nHCP fraction. The strong interactions between CG matrix and nHCP consume some hydrophilic groups and depress the water uptake. Moreover, the high hydrophilicity of pectin in nHCP result in the water absorption ability of nHCP/CG (50 wt%) being higher than that of nHA/CG (50 wt%).

The scaffolds are expected to be degradable and absorbable with a proper rate to match the speed of new tissues formation. The degradation behaviors of biomaterials in physiological environments play important roles in the engineering process of a new tissue. The degradation behaviors of nHCP/CG and nHA/CG 3D porous scaffolds in lysozyme PBS solution are shown in Fig. 4. These scaffolds' weight losses increased gradually during the whole period. The weight losses of nHCP/CG are lower than those of pure CG. The fraction of nHA crystals in nHCP with low degradation rate and low water absorption ability protected the CG matrix of nHCP/CG scaffold from hydrolyzing. Meanwhile, the degradation rate slowed down when the nHCP content increased (Fig. 4(A)). These phenomena may be due to the presence of nHCP providing chemical crosslinking sites, which enhance the stability of the network (Haroun, Gamal-Eldeen, & Harding, 2009). It indicated that the degradation behavior could be adjusted by changing the nHCP content in nHCP/CG scaffold. Moreover, the weight remaining of nHA/CG (50%) scaffolds is lower than that of nHCP/CG (50 wt%) scaffolds (cf. Fig. 4(B)). Chemical crosslinking between nHCP and CG matrix makes the degradation rate of nHCP/CG scaffold decrease. nHA particles may migrate from nHA/CG scaffolds because there are only weak ionic/polar interactions and hydrogen bonds between nHA and CG matrix.

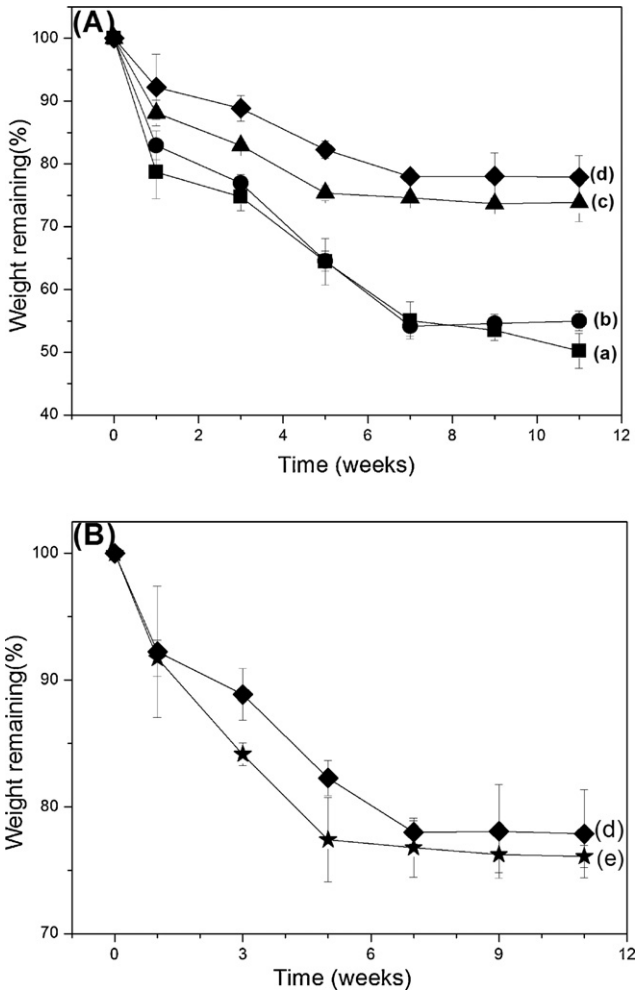

Fig. 4. Degradation behavior of CG, nHCP/CG and nHA/CG scaffolds in 0.1 M PBS containing 30,000 U/ml of lysozyme at 37 °C. Mean ± SD ($n = 5$). (a) CG, (b) nHCP/CG (10 wt%), (c) nHCP/CG (30 wt%), (d) nHCP/CG (50 wt%) and (e) nHA/CG (50 wt%).

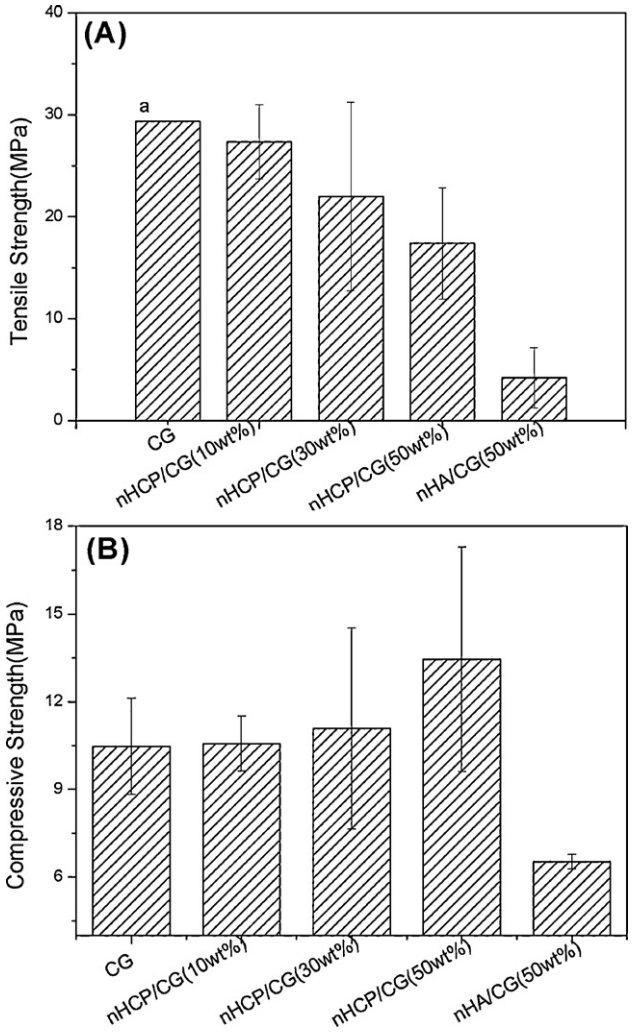

Fig. 5. (A) Tensile strength of CG, nHCP/CG and nHA/CG (50 wt%) films and (B) compressive strength of CG, nHCP/CG and nHA/CG (50 wt%) scaffolds (a: only one sample).

3.5. Mechanical behavior of nHCP/CG film and scaffold

Compared with CG films, nHCP/CG films exhibited lower tensile strength which decreased linearly with the increase of nHCP content. The tensile strength of nHCP/CG (50 wt%) films reached 17.40 ± 7.42 MPa. However, the tensile strength of nHA/CG (50 wt%) films is only 4.20 ± 2.90 MPa, as shown in Fig. 5(A). That is to say, the addition of naked nHA particles sharply weakens the tensile strength of CG films, but nHCP/CG film can maintain a higher tensile strength because there are amounts of flaws in nHA/CG films due to the heterogeneous dispersion and agglomeration of nHA particles in CG matrix. nHCP composites could uniformly combine into CG matrix due to the high stability of nHCP and chemical crosslinking between nHCP and CG matrix.

The compressive strength of scaffolds used is of particular importance in tissue engineering since they are closely linked to the dimension-maintaining ability and durability in practical operations and applications. The compressive performance is the necessity of the structural stability to withstand stress incurred during culturing in vitro and implanting in vivo (Pompe et al., 2003). Many factors can contribute to the mechanical response of the multicomponent composites scaffold, such as the particle sizes of the inorganic component, the inherent mechanical properties of the organic component, the interfacial interactions between the inorganic and organic components, the ratio of the inorganic/organic content and crosslinking character (Cai et al., 2009). Fig. 5(B) shows the result of the relationship between the contents of nHCP in nHCP/CG scaffolds and the compressive strength of the scaffold. Generally speaking, introducing nHCP into CG networks enhanced the compressive strength of scaffold. The compressive strength increased linearly with the increase of the nHCP content. The compressive strength of nHCP/CG (50 wt%) scaffold was 13.45 MPa. Comparing this with the data for human bone, the compressive strength of the composite scaffold is still far from that of the cortical bone (strength of 130–180 MPa), but is close to the cancellous bone (strength of 4–12 MPa) (Kerin, Wisnom, & Adams, 1998), while the compressive strength of CG scaffold was only 10.47 MPa. It is well known that the introduction of rigid chain segment could improve the materials' mechanical strength. As a result, the compressive strength of nHCP/CG increases because of the addition of pectin. Moreover, the strong chemical crosslinking interactions between nHCP and CG matrix also improve the compressive strength of nHCP/CG composite scaffolds. Meanwhile, a decrease in scaffold porosity greatly enhances the mechanical properties (O'Shea & Miao, 2008). However, introducing nHA into the CG scaffold greatly decreased the compressive strength of the nHA/CG scaffolds. The compressive strength of nHA/CG (50 wt%) scaffolds is only 6.53 MPa. The introduction of HA which is more brittle than CG would certainly increase the brittleness of nHA/CG composite scaffolds, leading to a corresponding decrease in their compressive

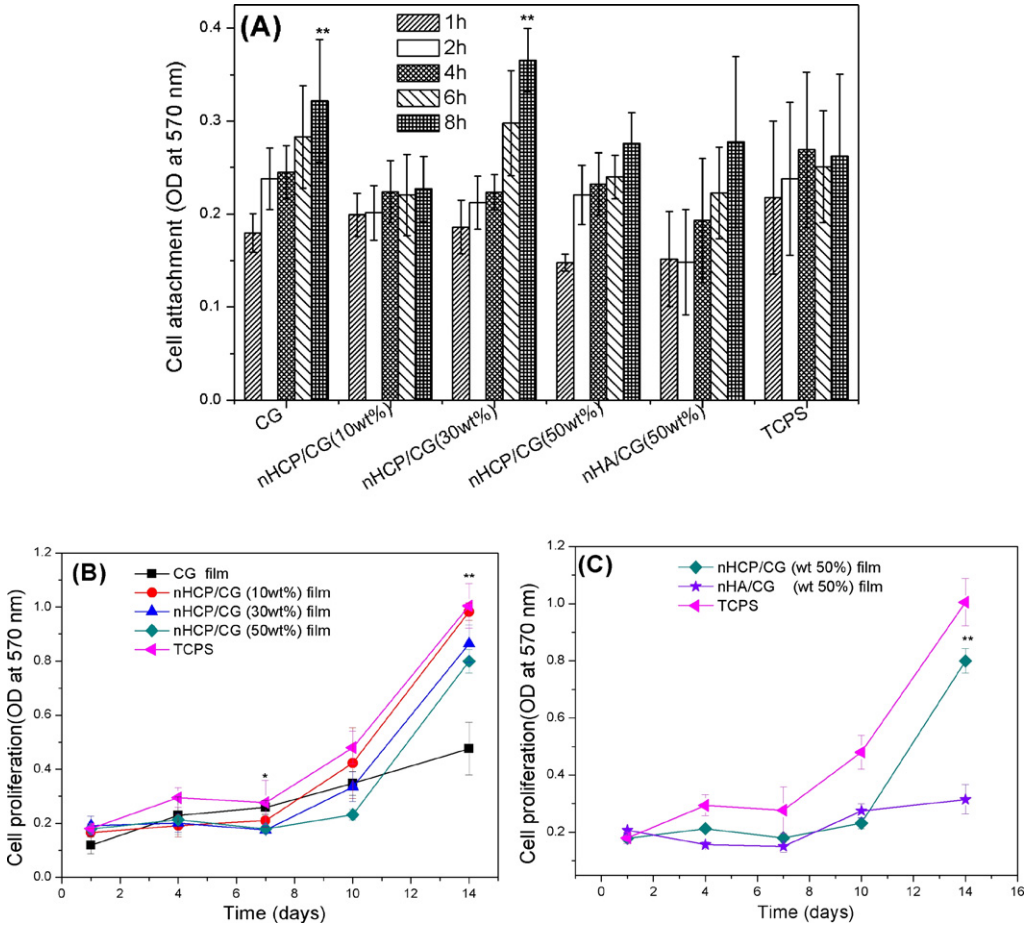

Fig. 6. The behavior of MC 3T3-E1 seeded on the CG, nHCP/CG, nHA/CG (50 wt%) films and TCPS. (A) Attachment characterics of MC 3T3-E1 over a 8 h period, cells were seeded initially at a density of 1.0×10^4 cells/ml. (B) and (C) Proliferation levels of MC 3T3-E1 over a 14-day period. Cells were seeded initially at a density of 1.0×10^4 cells/ml. ($^{**}p < 0.01$) were observed on nHCP/CG and nHA/CG with respect to CG.

strength (Teng et al., 2009). Furthermore, agglomeration of nHA crystals may occurred in nHA/CG composite scaffolds, larger sized nHA cyrstal acted as "flaws" in the continuous CG matrix due to the weak interactions between naked nHA and CG matrix (Wang, Song, & Lou, 2010).

3.6. Response of pre-osteoblasts (MC 3T3-E1) to nHCP/CG composite

3.6.1. Cell behaviors on nHCP/CG film

The scaffold used for bone tissue engineering should be non-toxic and have good biocompatibility, which is a central criterion for ultimately deciding the feasibility of implantation in body. The cell attachment and proliferation ability in scaffold in vitro is often employed as an important initial evaluation of cell biocompatibility. The attachment and proliferation of cells on scaffolds are complicated processes which are affected by many material factors, such as physical, chemical and geometric properties (Lieb et al., 2003). The nHCP/CG composites are composed of well biocompatible nHA and polysaccharide/protein which are expected to provide appropriate microenvironment that will modulate the cell attachment and proliferation. In order to understand the effect of chemical composition of nHCP/CG composites on cells behaviors of MC 3T3-E1, MC 3T3-E1 were seeded on nHCP/CG and nHA/CG films. Fig. 6(A) showed the attachment behaviors of MC 3T3-E1 cultured on the surfaces of nHCP/CG, nHA/CG (50 wt%) films and TCPS for a period of 8 h. More MC 3T3-E1 attached on nHCP/CG film surface than that on nHA/CG (50 wt%) surface with $p < 0.05$ at each time point. However, there is no significant difference in comparison with the TCPS. Moreover, the MC 3T3-E1 on nHCP/CG (30 wt%) showed the best attachment ability. Fig. 6(B) and (C) illustrated the MTT assay in terms of formosan absorbance as a measure of proliferation viability of pre-osteoblast seeded onto nHCP/CG and nHA/CG (50 wt%) films after 14 days culture. The result reveals that the cell proliferated with the culture time on both groups, but the growth rate of MC 3T3-E1 on the nHCP/CG film is much higher than those on CG film. The proliferation behaviors of MC 3T3-E1 pre-osteoblasts on nHCP/CG film are similar to that on TCPS (Fig. 6(B)). The chemical composition is an important factor that influences the cell behaviors. Chitosan exhibits high cell adhesion ability, while it restricts cell spreading, migration and proliferation due to the extremely high adhesion ability (Chupa, Foster, Sumner, Madihally, & Matthew, 2000; Hamilton et al., 2006). Our previous research also revealed the inhibition of cell proliferation on chitosan scaffolds (Mao et al., 2004). Furthermore, the hydrophilic pectin of nHCP/CG is suitable for cell proliferation as well supply of nutrients (Li, Kommareddy, et al., 2010; Li, Zhu, et al., 2010). It may not only bind peptides, including growth factors, which increase the effective concentration of these factors at the cell surface, but also attract integrins to the cell surface. On the other hand, the nHA (15.8 nm) crystals could also help the MC 3T3-E1 osteoblast, which carry calcium-sensing receptors and recognize the nHCP/CG microenvironment (Ye et al., 2000). Therefore, MC 3T3-E1 seeded on CG films showed lower proliferation activity than that on nHCP/CG. The nHCP/CG could maintain stable chemical composition during cell culture due to the chem-

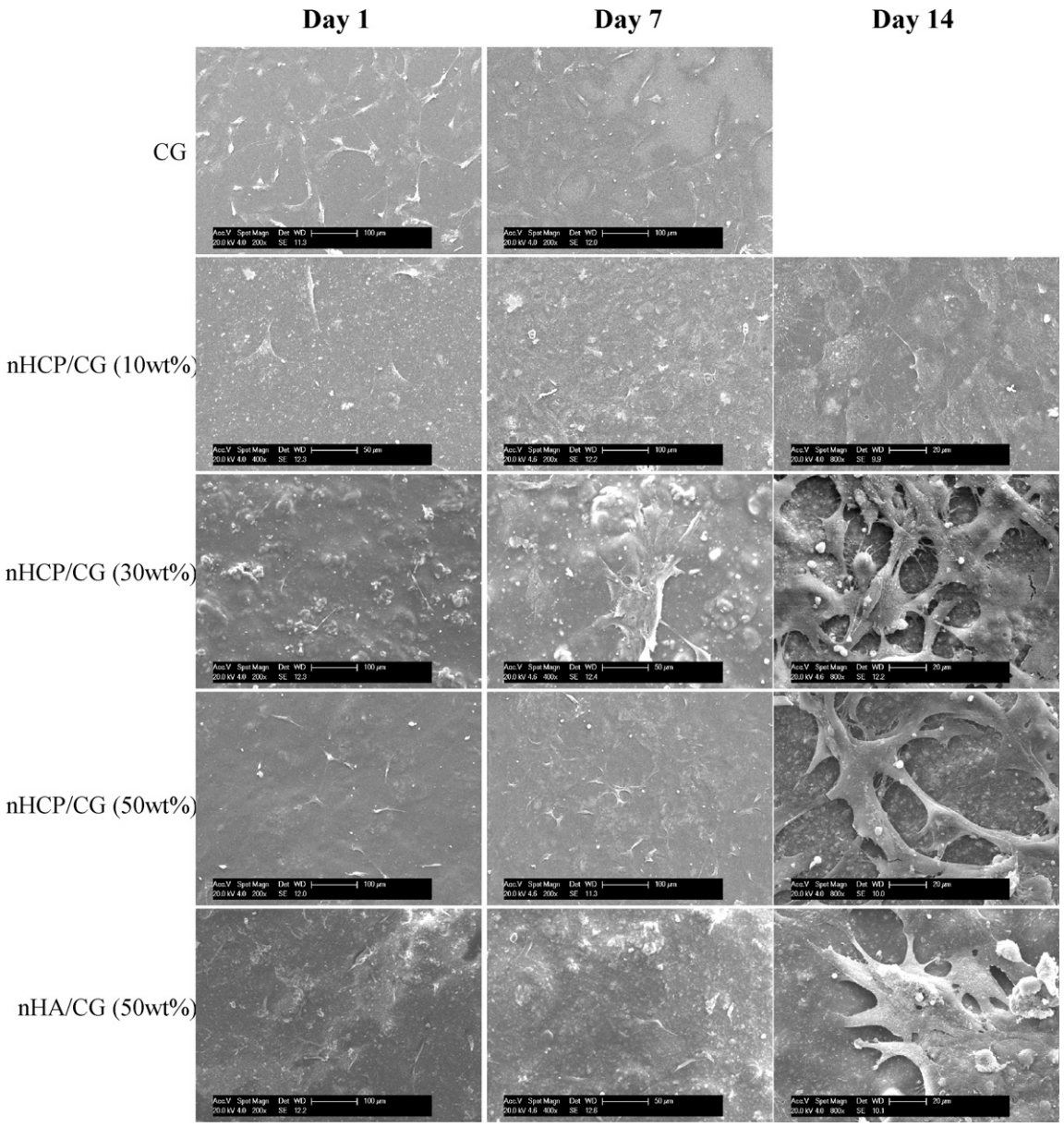

Fig. 7. SEM images of MC 3T3-E1 seeded on CG, nHCP/CG and nHA/CG (50 wt%) films cultured for 1, 7 and 14 days.

ical crosslinking. The agglomerated nHA particles could migrate from the nHA/CG film with the degradation of CG matrix, which makes some MC 3T3-E1 detached from the nHA/CG film. Therefore, MC 3T3-E1 cultured on nHCP/CG (50 wt%) films display significant differences compared with nHA/CG (50 wt%) films ($p < 0.01$) (Fig. 6(C)).

SEM images of pre-osteoblasts seeded on nHCP/CG and nHA/CG (50 wt%) films after 1, 7 and 14 days are presented in Fig. 7. In general, pre-osteoblasts attached, spread and grew well. Their morphology changed with time, irrespective of the type of film. At day 1, most of cells cultured on CG films were polygonal in shape while spindle cells appeared on other film surface. The morphology of pre-osteoblast on nHCP/CG (30 wt%), nHCP/CG (50 wt%) and nHA/CG (50 wt%) showed highly motility with filopodia and had the resemblance of a sheet at day 14. While, the flat pre-osteoblasts could be observed on nHCP/CG (10 wt%) film. On the other hand, the cell morphology seeded on CG was difficult to observe via SEM after 14 days because of the high degradation rate of CG film. Above results suggested that the nHCP/CG composites could construct appropriate microenvironment for the attachment and proliferation of MC 3T3-E1 pre-osteoblast.

3.6.2. Cell behaviors on nHCP/CG scaffold

The proliferation ability of pre-osteoblasts seeded in nHCG/CG (50 wt%) scaffold is significantly stronger than that in nHA/CG (50 wt%) scaffold within 21 days (Fig. 8(A)) The fluorescent photographs also showed the same results, as showed in Fig. 8(B) and (D). It can be observed clearly that the amount of MC 3T3-E1 increased a lot after 14 days culture compared with those cultured for 7 days. The cells were proliferating not only on the outer surface, but also inside the micropores. At day 14, the cells already began to grow around the corner of the pores, and multilayers of cells were visible. Furthermore, the pre-osteoblasts grew in a circular channel towards the interior of the pore channel. The pores were rounded by the cells and the diameter is ca. 130 μm. The same results can be found out from the SEM images (Fig. 8(C)).

Owing to the strong chemical crosslinking interactions between nHCP and CG network, the nHCP/CG scaffold could keep a constant composition to provide appropriate and steady chemical microen-

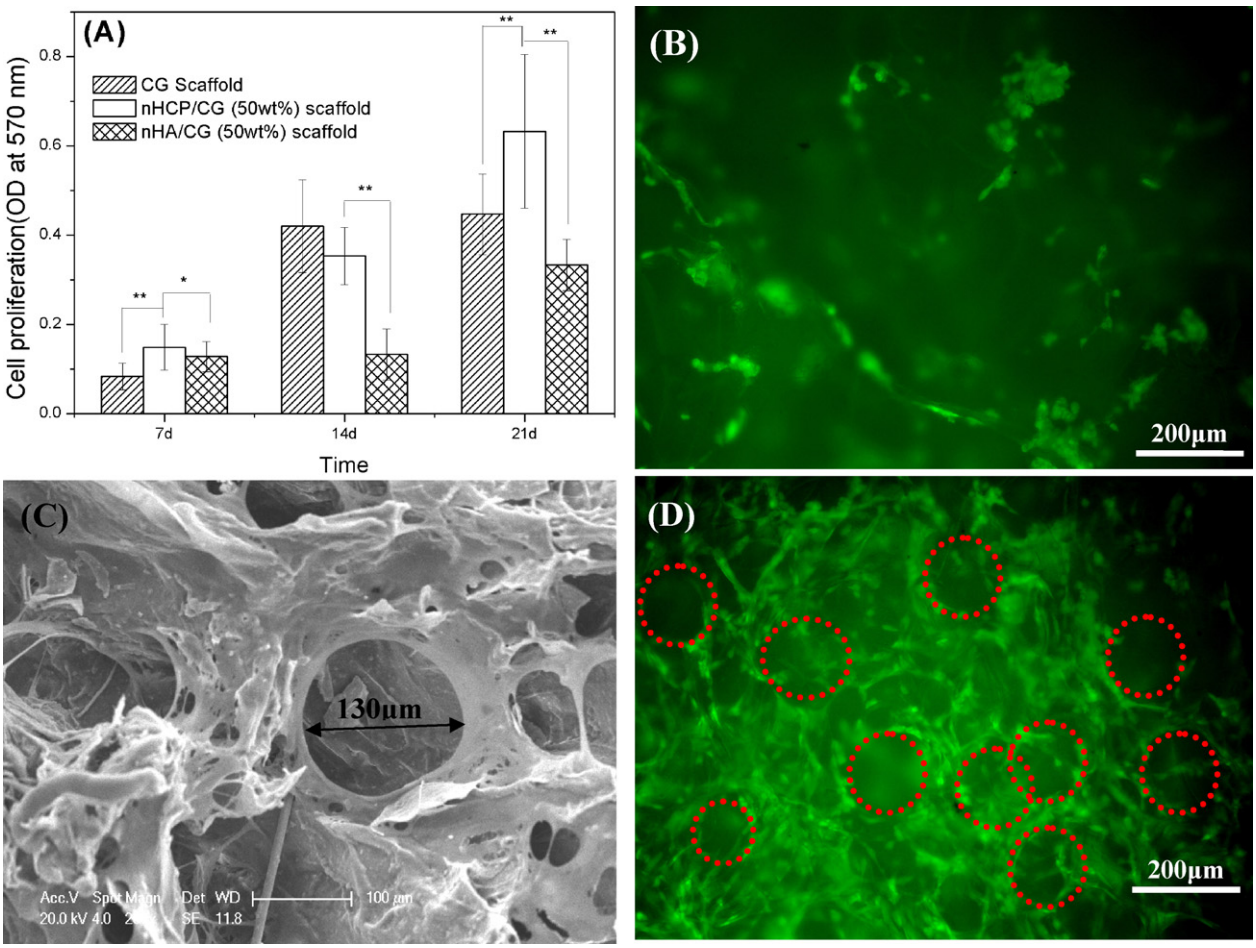

Fig. 8. The behaviors of MC 3T3-E1 seeded in CG, nHCP/CG (50 wt%) and nHA/CG (50 wt%) scaffold; (A) proliferation levels of MC 3T3-E1 within 21 days ($^{*}p < 0.05$, $^{**}p < 0.01$); (B) fluorescence micrographs of MC 3T3-E1 seeded in nHCP/CG (50 wt%) scaffold for 7 days; (C) SEM and (D) fluorescence micrographs of MC 3T3-E1 seeded in nHCP/CG (50 wt%) scaffolds for 14 days.

vironment for cell proliferation in a certain period. However, for nHA/CG scaffold, the chemical microenvironment of cell proliferation may be destroyed when nHA particles migrate from CG matrix. Moreover, nHCP/CG scaffolds could maintain their original shapes and keep enough pore space due to their high mechanical properties. The in vitro experiments showed that the nHCP/CG scaffolds possess sufficient mechanical strength that will maintain its shape after several weeks' culture of MC 3T3-E1 pre-osteoblast, which could provide appropriate physical microenvironment for cell attachment and proliferation. However the shape of CG composites was destroyed due to high degradation rate. As a result of the cooperating of these factors, nHCP/CG composites could improve the attachment and proliferation of MC 3T3-E1 pre-osteoblast.

4. Conclusions

In this article, the multicomponent polysaccharide/nano-hydroxyapatite composites (nHCP/CG) were reported. The nHCP/CG scaffolds which were prepared via mineralization and blending can mimic both nanoscale architecture and chemical composition of natural bone ECMs. The nHCP/CG scaffolds exhibited high porosity, interconnectivity, water absorption ability, controllable degradation behaviors and good mechanical strength. Furthermore, the nHCP/CG scaffolds also showed excellent mechanical stability and biocompatibility. This significantly improved biological responses of pre-osteoblast (MC 3T3-E1) to nHCP/CG included improved cell attachment, proliferation and morphology in compare with CG and nHA/CG composites. Especially for nHCP/CG (50 wt%) scaffold, the cell layer channels with ca. 130 μm formed after 14 days of cultivation. The nHCP/CG scaffolds avoided the agglomeration and migration of nHA particles in nHA/CG scaffolds due to the chemical crosslinking interactions between nHCP and CG matrix. In conclusion, the above results indicated that the biodegradable nHCP/CG scaffold with a desirable physico-chemical and biological properties will meet the essential requirement for bone tissue engineering.

Acknowledgements

This work has been supported in part by National Nature Science Foundation of China 51073119 and 50773050; Hebei Provincial Office of Public Health Foundation Key Project (20090549). The Programme of Introducing Talents of Discipline to Universities, no. B060006.

References

Cai, X., Tong, H., Shen, X. Y., Chen, W. X., Yan, J., & Hu, J. M. (2009). Preparation and characterization of homogeneous chitosan-polylactic acid/hydroxyapatite nanocomposite for bone tissue engineering and evaluation of its mechanical properties. *Acta Biomaterialia*, *5*(7), 2693–2703.

Cheng, X. M., Li, Y. B., Zuo, Y., Zhang, L., Li, J. D., & Wang, H. A. (2009). Properties and in vitro biological evaluation of nano-hydroxyapatite/chitosan membranes for bone guided regeneration. *Materials Science and Engineering C: Biomimetic and Supramolecular Systems*, *29*(1), 29–35.

Chupa, J. M., Foster, A. M., Sumner, S. R., Madihally, S. V., & Matthew, H. W. T. (2000). Vascular cell responses to polysaccharide materials: In vitro and in vivo evaluations. *Biomaterials*, *21*(22), 2315–2322.

Cui, F. Z., Li, Y., & Ge, J. (2007). Self-assembly of mineralized collagen composites. *Materials Science and Engineering R: Reports*, *57*(1–6), 1–27.

Di Martino, A., Sittinger, M., & Risbud, M. V. (2005). Chitosan: A versatile biopolymer for orthopaedic tissue-engineering. *Biomaterials*, *26*(30), 5983–5990.

Hamilton, V., Yuan, Y., Rigney, D. A., Puckett, A. D., Ong, J. L., Yang, Y., et al. (2006). Characterization of chitosan films and effects on fibroblast cell attachment and proliferation. *Journal of Materials Science: Materials in Medicine*, *17*(12), 1373–1381.

Haroun, A. A., Gamal-Eldeen, A., & Harding, D. R. K. (2009). Preparation, characterization and in vitro biological study of biomimetic three-dimensional gelatin-montmorillonite/cellulose scaffold for tissue engineering. *Journal of Materials Science: Materials in Medicine*, *20*(12), 2527–2540.

Kerin, A. J, Wisnom, M. R., & Adams, M. A. (1998). The compressive strength of articular cartilage. *Proceedings of the Institution of Mechanical Engineers H: Journal of Engineering in Medicine*, *212*(H4), 273–280.

Khor, E., & Lim, L. Y. (2003). Implantable applications of chitin and chitosan. *Biomaterials*, *24*(13), 2339–2349.

Kim, H. W., Kim, H. E., & Salih, V. (2005). Stimulation of osteoblast responses to biomimetic nanocomposites of gelatin-hydroxyapatite for tissue engineering scaffolds. *Biomaterials*, *26*(25), 5221–5230.

Kim, H. W., Knowles, J. C., & Kim, H. E. (2005). Hydroxyapatite and gelatin composite foams processed via novel freeze-drying and crosslinking for use as temporary hard tissue scaffolds. *Journal of Biomedical Materials Research A*, *72A*(2), 136–145.

Kokkonen, H., Cassinelli, C., Verhoef, R., Morra, M., Schols, H. A., & Tuukkanen, J. (2008). Differentiation of osteoblasts on pectin-coated titanium. *Biomacromolecules*, *9*(9), 2369–2376.

Li, J. J., Chen, Y. P., Yin, Y. J., Yao, F. L., & Yao, K. D. (2007). Modulation of nano-hydroxyapatite size via formation on chitosan–gelatin network film in situ. *Biomaterials*, *28*(5), 781–790.

Li, J. J., Dou, Y., Yang, J., Yin, Y. J., Zhang, H., Yao, F. L., et al. (2009). Surface characterization and biocompatibility of micro- and nano-hydroxyapatite/hitosan–gelatin network films. *Materials Science and Engineering C: Biomimetic and Supramolecular Systems*, *29*(4), 1207–1215.

Li, L. H., Kommareddy, K. P., Pilz, C., Zhou, C. R., Fratzl, P., & Manjubala, I. (2010). In vitro bioactivity of bioresorbable porous polymeric scaffolds incorporating hydroxyapatite microspheres. *Acta Biomaterialia*, *6*(7), 2525–2531.

Li, J. J., Zhu, D. W., Yin, J. W., Liu, Y. X., Yao, F. L., & Yao, K. D. (2010). Formation of nano-hydroxyapatite crystal in situ in chitosan–pectin polyelectrolyte complex network. *Materials Science and Engineering C: Materials for Biological Applications*, *30*(6), 795–803.

Lieb, E., Tessmar, J., Hacker, M., Fischbach, C., Rose, D., Blunk, T., et al. (2003). Poly(D,L-lactic acid)-poly(ethylene glycol)-monomethyl ether diblock copolymers control adhesion and osteoblastic differentiation of marrow stromal cells. *Tissue Engineering B: Review*, *9*(1), 71–84.

Liu, L. S., Fishman, M. L., Kost, J., & Hicks, K. B. (2003). Pectin-based systems for colon-specific drug delivery via oral route. *Biomaterials*, *24*(19), 3333–3343.

Liu, L. S., Won, Y. J., Cooke, P. H., Coffin, D. R., Fishman, M. L., Hicks, K. B., et al. (2004). Pectin/poly(lactide-co-glycolide) composite matrices for biomedical applications. *Biomaterials*, *25*(16), 3201–3210.

Mandal, B. B., Priya, A. S., & Kundu, S. C. (2009). Novel silk sericin/gelatin 3-D scaffolds and 2-D films: Fabrication and characterization for potential tissue engineering applications. *Acta Biomaterialia*, *5*(8), 3007–3020.

Manjubala, I., Ponomarev, I., Wilke, I., & Jandt, K. D. (2008). Growth of osteoblast-like cells on biomimetic apatite-coated chitosan scaffolds. *Journal of Biomedical Materials Research B: Applied Biomaterials*, *84B*(1), 7–16.

Manjubala, I., Scheler, S., Bossert, J., & Jandt, K. D. (2006). Mineralisation of chitosan scaffolds with nano-apatite formation by double diffusion technique. *Acta Biomaterialia*, *2*(1), 75–84.

Mao, J. S., Cui, Y. L., Wang, X. H., Sun, Y., Yin, Y. J., Zhao, H. M., et al. (2004). A preliminary study on chitosan and gelatin polyelectrolyte complex cytocompatibility by cell cycle and apoptosis analysis. *Biomaterials*, *25*(18), 3973–3981.

Nejati, E., Firouzdor, V., Eslaminejad, M. B., & Bagheri, F. (2009). Needle-like nano hydroxyapatite/poly(L-lactide acid) composite scaffold for bone tissue engineering application. *Materials Science and Engineering C: Biomimetic and Supramolecular Systems*, *29*(3), 942–949.

O'Shea, T. M., & Miao, X. (2008). Bilayered scaffolds for osteochondral tissue engineering. *Tissue Engineering B: Review*, *14*(4), 447–464.

Pompe, W., Worch, H., Epple, M., Friess, W., Gelinsky, M., Greil, P., et al. (2003). Functionally graded materials for biomedical applications. *Materials Science and Engineering A: Structural Materials Properties Microstructure and Processing*, *362*(1–2), 40–60.

Rohanizadeh, R., Swain, M. V., & Mason, R. S. (2008). Gelatin sponges (Gelfoam (R)) as a scaffold for osteoblasts. *Journal of Materials Science: Materials in Medicine*, *19*(3), 1173–1182.

Suh, J. K. F., & Matthew, H. W. T. (2000). Application of chitosan-based polysaccharide biomaterials in cartilage tissue engineering: A review. *Biomaterials*, *21*(24), 2589–2598.

Teng, S. H., Lee, E. J., Yoon, B. H., Shin, D. S., Kim, H. E., & Oh, J. S. (2009). Chitosan/nanohydroxyapatite composite membranes via dynamic filtration for guided bone regeneration. *Journal of Biomedical Materials Research A*, *88A*(3), 569–580.

Thein-Han, W. W., & Misra, R. D. K. (2009). Biomimetic chitosan-nanohydroxyapatite composite scaffolds for bone tissue engineering. *Acta Biomaterialia*, *5*(4), 1182–1197.

Wang, X., Song, G., & Lou, T. (2010). Fabrication and characterization of nano composite scaffold of poly(L-lactic acid)/hydroxyapatite. *Journal of Materials Science: Materials in Medicine*, *21*(1), 183–188.

Ye, C. P., Yamaguchi, T., Chattopadhyay, N., Sanders, J. L., Vassilev, P. M., & Brown, E. M. (2000). Extracellular calcium-sensing-receptor (CaR)-mediated opening of an outward K^+ channel in murine MC3T3-E1 osteoblastic cells: Evidence for expression of a functional CaR. *Bone*, *27*(1), 21–27.

Yin, Y. J., Luo, X. Y., Cui, J. F., Wang, C. Y., Guo, X. M., & Yao, K. D. (2004). A study on biomineralization behavior of N-methylene phosphochitosan scaffolds. *Macromolecular Bioscience*, *4*(10), 971–977.

Zhao, F., Yin, Y. J., Lu, W. W., Leong, J. C., Zhang, W. J., Zhang, J. Y., et al. (2002). Preparation and histological evaluation of biomimetic three-dimensional hydroxyapatite/chitosan–gelatin network composite scaffolds. *Biomaterials*, *23*(15), 3227–3234.